Mass Diffusion Coefficients of Cellulose Acetate Butyrate in Methyl Ethyl Ketone Solutions at Temperatures between (293 and 323) K and Mass Fractions from 0.05 to 0.60 Using the Soret Forced Rayleigh Scattering Method†

Maiko Niwa, Yuzo Ohta, and Yuji Nagasaka*

Department of System Design Engineering, Keio University, 3-14-1, Hiyoshi, Yokohama 223-8522, Japan

The binary mass diffusion coefficients of cellulose acetate butyrate in methyl ethyl ketone solutions (CAB + MEK) have been measured under atmospheric pressure at temperatures from (293 to 323) K and mass fractions from 0.05 to 0.6. The present experimental apparatus is based on the Soret forced Rayleigh scattering method (S-FRSM), which utilizes the Soret effect to create periodic spatial concentration modulation of micrometer-order fringe spacing in a sample binary liquid mixture due to the absorption of an optical interference grating generated by two intersecting heating laser beams. The decay of the concentration modulation by the mass diffusion process is monitored by the diffraction of a probing laser beam. This method provides several advantages in comparison with conventional techniques such as Taylor dispersion or diaphragm cells; namely, a single measurement can be performed within a short time [(10^{-3} to 10^{-2}) s], with small temperature and concentration changes ($\Delta T < 10^{-2}$ K and $\Delta c < 10^{-5}$) using a microliter-order sample volume. To check the reliability of S-FRSM to measure mass diffusion coefficients, the mass diffusion coefficients of toluene + *n*-hexane, ethanol + benzene, and acetone + carbon tetrachloride were also measured. The expanded ($k = 2$) uncertainty in mass diffusion coefficients for CAB + MEK solutions is estimated to be within ± 3.6 %.

Introduction

To control the internal microstructure of highly functional polymeric films such as optical films, it is important to know as much as possible about the thermophysical properties of the polymer solutions such as surface tension, viscosity, and mass diffusion coefficient of the polymer solutions because such polymeric films are produced through the drying of dilute polymer organic−solvent systems in the case of the wet coating process.[1] In the latter portion of the drying process, the process is primarily governed by mass diffusion in concentrated solutions, resulting in diffusion-limited evaporation.[2] Consequently, the mass diffusion coefficients of constituent polymer solutions for the films are required as a function of temperature and concentration especially for the elevated region.[3] Even though, in the case of polystyrene in toluene concentrated solutions, a critical assessment of diverging experimental results for mass diffusion coefficient can be found in a very recent paper,[4] this should be treated as an exceptional case. From an experimental point of view, it is difficult to apply conventional techniques like Taylor dispersion and dynamic light scattering to measure the mass diffusion coefficients of those polymer solutions due to their large viscosity and small diffusion coefficients. Since almost no experimental data on mass diffusion coefficients for these polymer solutions are available in the literature, semiempirical prediction models have been employed to obtain those values.[5]

The Soret forced Rayleigh scattering method (S-FRSM) is one of the highly complementary techniques to the Taylor dispersion method for the measurement of binary liquid mixtures with high viscosity and a low mass diffusion coefficient. The first Soret forced Rayleigh scattering experiment was started by Thyagarajan and Lallemand,[6] who measured the thermal diffusion ratio of a carbon disulfide/ethanol mixture. Subsequently, Pohl[7] demonstrated the possibility of applying the technique to study the phase separation of binary liquid mixtures. Somewhat later, Köhler and co-workers[8,9] showed that the Soret forced Rayleigh scattering method (or thermal diffusion forced Rayleigh scattering) provides a useful and sensitive tool for the investigation of thermal diffusion in polymer solutions. Butenhoff et al.[10] used this same technique to determine the mass diffusion coefficients of concentrated hydrothermal $NaNO_3$ solutions under high-temperature, high-pressure conditions.

In our laboratory at Keio University, we have developed a measurement theory and experimental apparatus to measure the thermal diffusivity of liquids by the forced Rayleigh scattering method[11] and reported the measurements of high-temperature molten salts.[12] In parallel with the study for the thermal diffusivity measurement using forced Rayleigh scattering, we have developed a Soret forced Rayleigh scattering apparatus to measure mass diffusion coefficients of polymer solutions and fullerene solutions.[13−15] In the present paper, we have modified and applied our Soret forced Rayleigh scattering apparatus to measure the binary mass diffusion coefficient of cellulose acetate butyrate (CAB) in methyl ethyl ketone (MEK) solutions at temperatures between (293 and 323) K and mass fractions from 0.05 to 0.60. CAB is soluble in low molecular weight alcohols as well as other common organic solvents and is widely used in the manufacture of highly functional polymer films.[16−18]

Theory

Figure 1 schematically shows the principle and ideal signal waveform of the Soret forced Rayleigh scattering method to

* Corresponding author. Tel. and Fax: +81-45-566-1735. E-mail: nagasaka@sd.keio.ac.jp.

† Part of the "William A. Wakeham Festschrift".

10.1021/je900242e CCC: $40.75
Published on Web 05/29/2009

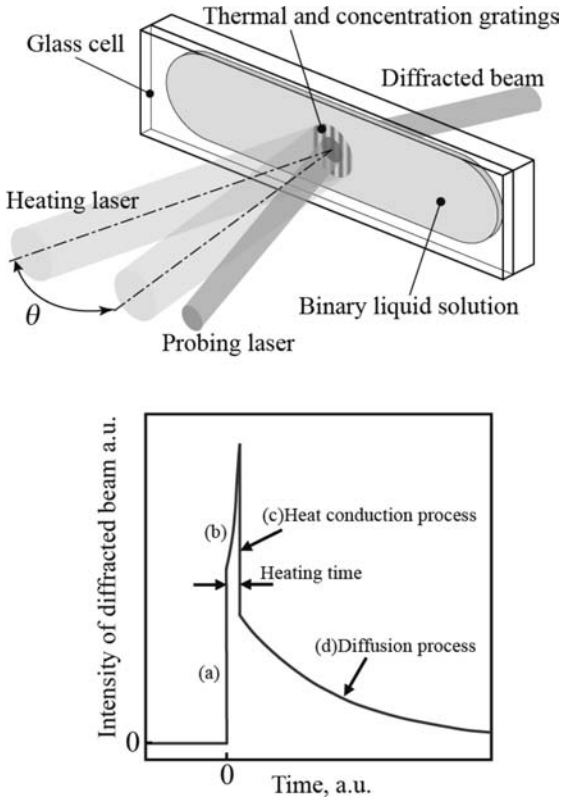

Figure 1. Top: principle of the Soret forced Rayleigh scattering method for measuring the mass diffusion coefficient of a binary liquid solution. Bottom: ideal signal waveform of diffracted beam intensity. (a) Generation of thermal grating; (b) generation of concentration grating; (c) decay of diffracted beam intensity due to heat conduction (determination of thermal diffusivity); and (d) decay of diffracted beam intensity due to mass diffusion (determination of mass diffusion coefficient).

determine the mass diffusion coefficient of a binary liquid solution. Pulses of two heating laser beams of equal intensity and wavelength are crossed at an angle θ in an absorbing sample solution filled in a glass cell. The optical interference of the two heating beams generates a spatially sinusoidal intensity modulation of fringe spacing Λ which induces a corresponding temperature distribution (thermal grating) in the x direction of the sample (process (a) in Figure 1). Then, an overlap of the concentration distribution (concentration grating) with the thermal grating is created, driven by the Soret effect (process (b) in Figure 1). Therefore, both the temperature and concentration modulation induce a spatial modulation of the index of refraction, at the heated area of the binary liquid solution, which acts as a volume diffraction grating on the probing laser beam, which is not absorbed by the sample. After the heating laser is switched off, simultaneous decay phenomena occur by heat conduction (process (c) in Figure 1) and mass diffusion (process (d) in Figure 1). Since normally the ratio between the thermal diffusivity a and the mutual mass diffusion coefficient D_{12} of liquids, or Lewis number, $a/D_{12} \approx 10^2 \sim 10^3$, it is possible to separately determine the thermal diffusivity and the mass diffusion coefficient by observing the two distinguishable decay time constants.

If the fringe spacing is small compared with the sample thickness, the sample absorption length, and the diameter of the heated area,[11] the assumption of one-dimensional heat conduction in the x direction is valid as

$$\frac{\partial T(x,t)}{\partial t} = a\frac{\partial^2 T(x,t)}{\partial x^2} + \frac{\alpha}{\rho C_p} I_h(x) \tag{1}$$

where α is the absorption coefficient at the wavelength of the heating beams; ρ is the density; and C_p is the specific heat at constant pressure of the solution. It is also assumed that the total absorption of the heating laser is weak ($\alpha \times$ sample thickness < 1), which implies an almost uniform instantaneous volume heating condition. $I_h(x)$ is the intensity within the interference zone of the sample produced by the two heating laser beams of equal intensity, $I_{h,0}/2$

$$I_h(x) = I_{h,0}(1 + \cos qx) \tag{2}$$

where $q = 2\pi/\Lambda$ is the wavenumber of the interference pattern. If the incidences of the two heating beams are symmetrical in relation to the normal direction of the sample surface, the relation between the fringe spacing Λ and the crossing angle of heating beams θ can be described by

$$\Lambda = \frac{\lambda_h}{2\sin(\theta/2)} \approx \frac{\lambda_h}{\theta} \; (\theta \approx 0) \tag{3}$$

where λ_h is the wavelength of the heating beam. The solution to eqs 1 and 2 is

$$T(x,t) = T_m(t) + \Delta T(t)\cos qx + T_0 \tag{4}$$

where $\Delta T(t)$ is the spatial temperature amplitude during laser heating

$$\Delta T(t) \equiv \frac{\alpha I_{h,0}}{\rho C_p}\tau_a\left\{1 - \exp\left(\frac{-t}{\tau_a}\right)\right\} \tag{5}$$

τ_a is the decay time constant of heat conduction

$$\tau_a = \frac{1}{aq^2} = \frac{1}{a}\left(\frac{\Lambda}{2\pi}\right)^2 \tag{6}$$

T_0 is the initial uniform temperature, and $T_m(t)$ is the mean temperature rise of the sample in the course of laser heating

$$T_m(t) = \frac{\alpha I_{h,0}}{\rho C_p} t \tag{7}$$

It should be noted that, at first, we define the time at the start of heating as $t = 0$ to describe the time evolution of temperature and concentration gratings illustrated in Figure 1(a) and (b).

The temperature distribution described by eq 4 is coupled to create a concentration distribution due to the Soret effect governed by the following one-dimensional diffusion equation[19]

$$\frac{\partial c(x,t)}{\partial t} = D_{12}\frac{\partial^2 c(x,t)}{\partial x^2} + D_T c(x,t)\{1 - c(x,t)\}\frac{\partial^2 T(x,t)}{\partial x^2} \tag{8}$$

where $c(x,t)$ is the solute mole fraction; D_{12} ($m^2 \cdot s^{-1}$) is the mutual mass diffusion coefficient; and D_T ($m^2 \cdot s^{-1} \cdot K^{-1}$) is the thermal diffusion coefficient, which is defined to be positive if the solute migration due to thermal diffusion is from regions of high temperature to low temperature. Consequently, the spatial and temporal behavior of the concentration grating is derived by substituting eq 4 into eq 8. Assuming small concentration changes during the heating, $c(x,t)\{1 - c(x,t)\} \approx c_0$, with c_0 being the initial uniform concentration of the solute, and the solution is given by[8]

$$c(x,t) = \frac{\alpha I_{h,0}}{\rho C_p}\frac{D_T}{(a - D_{12})}c_0\left[\tau_a\left\{1 - \exp\left(\frac{-t}{\tau_a}\right)\right\} - \tau_D\left\{1 - \exp\left(\frac{-t}{\tau_D}\right)\right\}\right]\cos qx + c_0 \quad (9)$$

where τ_D is the decay time constant of mass diffusion

$$\tau_D = \frac{1}{D_{12}q^2} = \frac{1}{D_{12}}\left(\frac{\Lambda}{2\pi}\right)^2 \quad (10)$$

Since it is reasonable to assume $\tau_D \gg \tau_a$ ($D_{12} \ll a$) in the present liquid mixtures and we should set the heating laser duration time $t_h \gg \tau_a$ as shown in Figure 1 and also by substituting eqs 6 and 10, at $t \sim t_h$, eq 9 can be sufficiently approximated by

$$c(x,t) = -\frac{\alpha I_{h,0}}{\rho C_p}S_T c_0 \tau_a\left\{1 - \exp\left(\frac{-t}{\tau_D}\right)\right\}\cos qx + c_0 \quad (11)$$

where $S_T = D_T/D_{12}$ is the Soret coefficient. Equation 9 is rewritten as

$$c(x,t) = \Delta c(t)\cos qx + c_0 \quad (12)$$

$$\Delta c(t) \equiv -\frac{\alpha I_{h,0}}{\rho C_p}S_T c_0 \tau_a\left\{1 - \exp\left(\frac{-t}{\tau_D}\right)\right\} \quad (13)$$

To describe the decay processes, from which we practically determine the thermal diffusivity and the mass diffusion coefficient, it is convenient to switch the definition of $t = 0$ to the time at the end of heating by making use of the ongoing derivations. Subsequent to the heating laser pulse duration time t_h, the thermal grating decays are expressed by the following equation

$$T(x,t) = T_m(t_h) + \Delta T(t_h)\exp\left(\frac{-t}{\tau_a}\right)\cos qx + T_0 \quad (14)$$

Then, the concentration grating exponentially decays with a much larger time constant $\tau_D \gg \tau_a$

$$c(x,t) = \Delta c(t_h)\exp\left(\frac{-t}{\tau_D}\right)\cos qx + c_0 \quad (15)$$

The spatially periodic temperature and concentration distributions produce a corresponding refractive index distribution which acts as an optical phase grating for the probing laser beam. The diffraction efficiency η in the case of the Bragg condition is expressed as[20]

$$\eta = \frac{I_1}{I_p} = \sin^2\left(\frac{\pi\Delta n(t)}{\lambda_p}d\right) \approx \left(\frac{\pi\Delta n(t)}{\lambda_p}d\right)^2 \propto \Delta n(t)^2 \quad (16)$$

Here, I_p is the intensity of the probing beam; I_1 is the intensity of the diffracted beam; λ_p is the wavelength of the probing beam; $\Delta n(t)$ is the amplitude of the refractive index at the wavelength of the probing beam; and d is the sample thickness. The above approximation is always valid due to the fact that $\pi\Delta n(t)d/\lambda_p \approx 10^{-5} \sim 10^{-6}$ in the present experimental conditions. For small temperature and concentration modulation, the amplitude of the refractive index is given by

$$\Delta n(t) = \Delta T(t)\frac{\partial n}{\partial T}(T_0, c_0) + \Delta c(t)\frac{\partial c}{\partial T}(T_0, c_0) \quad (17)$$

Substituting eqs 15 and 17 into eq 16, the final expression for the intensity of the diffracted beam during the mass diffusion process is found

$$I_1(t) = I_p\left(\frac{\pi d}{\lambda_p}\right)^2\left(\frac{\partial n}{\partial c}\right)^2\left[\frac{\alpha I_{h,0}}{\rho C_p}S_T c_0 \tau_a\left\{1 - \exp\left(\frac{-t_h}{\tau_D}\right)\right\} \times \exp\left(\frac{-t}{\tau_D}\right)\right]^2 \quad (18)$$

$$I_1 \propto \exp\left(\frac{-2t}{\tau_D}\right) \quad (19)$$

Therefore, we are able to determine the mass diffusion coefficient D_{12} by measuring the decay time constant τ_D and the fringe spacing Λ.

Apparatus and Experimental Procedures

Apparatus. The experimental setup employed to perform the measurements is shown in Figure 2. A vertically polarized light beam of a single-mode CW argon−ion laser (NEC GLG3480) operating at a wavelength of 514.5 nm with a maximum power of 2.2 W and beam waist of 1.4 mm ($1/e^2$) was used as the heating source. The continuous light of the heating laser beam is modulated into short pulses of (0.1 to 20) ms by an acoustic optical modulator (Brimrose TEF-100) which is controlled by a function synthesizer (NF WF1956). The pulsed laser beam is split into two beams of equal intensity by a beam splitter, which is made to overlap at a small crossing angle θ in a sample to generate an interference pattern. In the present setup, the range of fringe spacing of the interference pattern is adjusted from about (4 to 9) μm, which corresponds to a beam crossing angle range of about 3.3° to 7.4°. The fringe spacing is measured by means of a laser beam profiler (Photon BeamScan) which works by moving a very narrow scanning slit across the beam in front of a photo detector to collect the irradiance profile.[21] In actual determination of the particular fringe spacing, we carefully place the scanhead of the laser beam profiler in the middle of the interference zone to acquire the number of sequential data points corresponding to 20 periods of fringe spacing with sampling resolution of ± 0.14 μm. By using the suitable curve fitting procedure for those data points, the expanded ($k = 2$) uncertainty in the fringe spacing is estimated to be ± 0.035 μm including other factors like possible small tilt angle of the scanhead against the direction of the grating vector and reproducibility of the scanning procedure.

The probing beam is produced by an 18 mW He−Ne laser (NEC GLG5400, wavelength of 632.8 nm) and is impinged into the interference zone of the sample at the Bragg angle. The diffracted probing beam is detected in the homodyne scheme by a photomultiplier tube (Hamamatsu R9110) through a pinhole and a high-pass filter (cutoff wavelength of 600 nm). The output

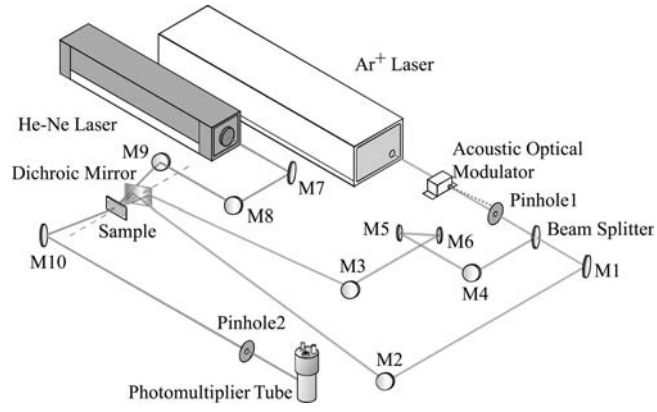

Figure 2. Experimental setup of the Soret forced Rayleigh scattering method.

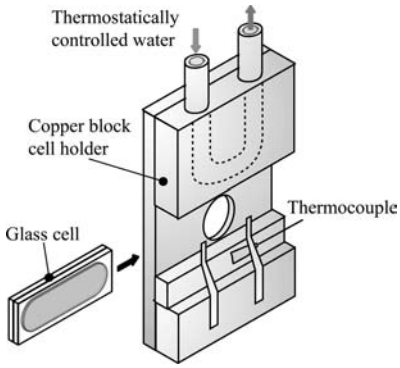

Figure 3. Sample cell together with the temperature-controlled cell holder.

signal is amplified by a variable gain current−voltage amplifier (FEMTO DLPCA-200) and is sent to a digital oscilloscope (Tektronix TDS3032B). The experiment is repeated at the same condition at intervals of 4 s which is considerably longer than the decay time constant of (10^{-4} to 10^{-2}) s in the present setup; usually, 16 waveforms are averaged to obtain a single mass diffusion coefficient measurement. The averaged waveform is then transferred to a computer for data analysis to determine the decay time constant of the mass diffusion process.

Since we have been adopting the homodyne detection to determine the mass diffusion decay time constant from the diffracted light signals, we have to arrange the measuring conditions so as to secure a sufficiently high light-signal intensity in comparison with the undesired but inevitable coherent scattered light from the cell window and from the sample itself.[11] The data analysis of the amplified output voltage $V(t)$, which is proportional to the detected light intensity by the photomultiplier tube, is carried out by the following equations and takes into account the coherent and incoherent scattered light superimposed over the diffracted light signal of interest

$$V(t) - V(\infty) = A \exp(-2t/\tau_D) + D \exp(-t/\tau_D) \tag{20}$$

with

$$D = 2\sqrt{AV(\infty)} \cos \psi \tag{21}$$

Here, A and D are the amplitude factors for the diffracted and the scattered light signals, respectively, and ψ is the phase difference between the diffracted light signal and the coherent scattered light. In eq 20, we also assume that at a time sufficiently larger than τ_D the measured background voltage shift $V(\infty)$ is proportional to the total scattered light. Actually, we adopted the procedure of picking out the measurement result having a threshold value $A/D \geq 10$ after extracting four fitting parameters, τ_D, A, D, and $V(\infty)$, out from $V(t)$ data by the simplex method.[22]

Figure 3 illustrates the sample cell together with a temperature controlled cell holder. The sample cell is essentially made out of two quartz glass plates (10 mm × 35 mm × 1 and 1.5 mm), and one side of a glass plate (thickness 1.5 mm) is etched with a depth of 0.5 mm. For samples with low viscosity polymer solutions, we simply put a drop of a very small amount of sample (about 175 μL) into the etched hollow area using a syringe, and then we cover the sample surface with another cover glass plate (thickness 1 mm). The interfacial tension between the sample and the glass plates ensures sufficient adhesion. We prepared two other types of sample cells depending on the viscosity of the sample; a cell with an additional screwed cap for volatile organic liquid mixtures and a cell with two joint glass tubes attached perpendicular to the cover glass plate to squeeze highly viscous polymer solutions into the sample cell. After filling the sample into the cell, the glass cell is fixed to a copper block cell holder, the temperature of which is controlled by the flow of water from a thermostat bath (Tokyo Rikakikai CTP-101) with a maximum flow rate of 8 L per minute. The temperature of the sample is measured by a K-type thermocouple with the uncertainty of ± 0.1 K.

Table 1. Mass Diffusion Coefficient D_{12} of Three Binary Liquid Mixtures Determined by the Soret Forced Rayleigh Scattering Method

system (1 + 2)	x_1[a]	T/K	$D_{12}/10^{-9}$ m^2·s^{-1}
toluene + *n*-hexane	0.250	298.15 ± 0.1	3.81 ± 0.010[b]
	0.500		2.84 ± 0.016
	0.750		2.66 ± 0.015
ethanol + benzene	0.0957	298.15 ± 0.1	1.20 ± 0.016
		313.15 ± 0.1	1.76 ± 0.004
	0.2034	298.15 ± 0.1	0.982 ± 0.009
		313.15 ± 0.1	1.39 ± 0.008
	0.3415	298.15 ± 0.1	0.932 ± 0.004
		313.15 ± 0.1	1.28 ± 0.008
	0.5068	298.15 ± 0.1	1.03 ± 0.054
		313.15 ± 0.1	1.43 ± 0.017
acetone + carbon tetrachloride	0.2056	298.15 ± 0.1	1.52 ± 0.017
	0.3942		1.67 ± 0.006
	0.7934		2.75 ± 0.019

[a] Mole fraction of component 1. [b] Standard deviation.

Assessment of Uncertainty. To check the reliability of the Soret forced Rayleigh scattering instrument used in the present study, we need reference data for the mass diffusion coefficient of binary liquid mixtures. At this time, no internationally agreed-upon reference data for liquid diffusion coefficients are available except for aqueous solutions of potassium chloride.[23] However, aqueous solutions of electrolytes are not an appropriate reference system for checking the operation of Soret forced Rayleigh scattering instruments because of their small Soret coefficients (S_T = (10^{-4} to 10^{-5}) K^{-1}), indicating the very weak driving force to create a concentration grating in the present technique (signal intensity ∝ S_T^2). We therefore selected three organic binary systems, namely, toluene + *n*-hexane, ethanol + benzene, and acetone + carbon tetrachloride, which have relatively large Soret coefficients {(10^{-2} to 10^{-3}) K^{-1}} with some reliable experimental studies of diffusion coefficients using different measurement techniques.

The toluene and ethanol used in the present work were supplied by Junsei Chemical, Ltd. and had a mass fraction purity better than 99.5 %. The *n*-hexane (Sigma-Aldrich Co.) had a purity of 99 %, and the carbon tetrachloride (Wako Pure Chemicals Industries, Ltd.) had a purity of 99.5 %. We used those chemicals without further purification. To prepare the bulk volume of mixtures (about 40 g in total), we first weighed each component with the uncertainty of 1 mg on a digital balance (Mettler Toledo XS205DU) having a resolution of 0.01 mg and then mixed the components in a clean glass bottle with a cap. For suitable energy absorption of the heating laser, all the mixtures were doped with 0.4 g·L^{-1} (equivalent to a mass fraction of 0.00028 to 0.00057 depending on the mixture) of quinizarin (1,4 dihydroxy-anthraquinone) which corresponds to an absorption coefficient of about 2000 m^{-1}. The effect of dye concentration on the measured mass diffusion coefficient for toluene/*n*-hexane as a reference system for organic solution was experimentally checked by adding quinizarine at four mass fractions of (0.00007, 0.00013, 0.00027, 0.00053, and 0.0008), and it was found that the agreement of these results was well

Table 2. Values of Coefficients a_{ij} in Equation 22

system (1 + 2)	a_{00}	a_{01}	a_{10}	a_{11}	a_{20}	a_{21}
toluene + *n*-hexane	$4.6060 \cdot 10^{-9}$	0	$-4.9501 \cdot 10^{-9}$	0	$2.9858 \cdot 10^{-9}$	0
ethanol + benzene	$2.3165 \cdot 10^{-10}$	$4.8718 \cdot 10^{-11}$	$3.5774 \cdot 10^{-10}$	$-1.4075 \cdot 10^{-10}$	$-2.4339 \cdot 10^{-11}$	$1.8791 \cdot 10^{-10}$
acetone + carbon tetrachloride	$1.6116 \cdot 10^{-9}$	0	$-1.1425 \cdot 10^{-9}$	0	$3.2485 \cdot 10^{-9}$	0

within the estimated uncertainty. We used a syringe to load the small amount of sample (175 μL) into the glass cell.

Table 1 lists the experimental results for the mass diffusion coefficient of (toluene + *n*-hexane), (ethanol + benzene), and (acetone + carbon tetrachloride). These values are the averages of two to five measurements at the same temperature under atmospheric pressure. In these measurements, the fringe spacing selected was (4.28 to 8.55) μm, depending on the measured mixtures, and the heating pulse duration time of the argon−ion laser was (0.5 to 1.5) ms with an output power of (0.5 to 1.5)

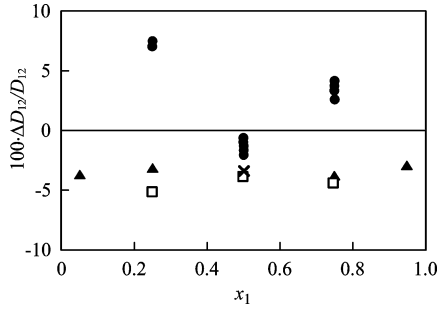

Figure 4. Fractional deviations $\Delta D_{12} = D_{12}(\text{exp}) - D_{12}(\text{corr})$ of the experimental mass diffusion coefficient D_{12}(exp) of toluene + *n*-hexane at $T = 278.15$ K from values D_{12}(corr) obtained with the correlation eq 22 with the coefficients in Table 3. ●, present work; □, ref 24; ×, ref 25; ▲, ref 26.

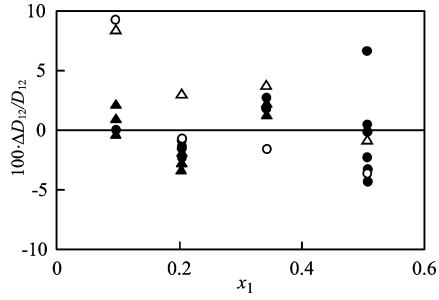

Figure 5. Fractional deviations $\Delta D_{12} = D_{12}(\text{exp}) - D_{12}(\text{corr})$ of the experimental mass diffusion coefficient D_{12}(exp) of ethanol + benzene from values D_{12}(corr) obtained with the correlation eq 22 with the coefficients in Table 3. ●, present work at $T = 298.15$ K; ○, ref 27 at $T = 298.15$ K; △, present work at $T = 313.15$ K; ▲, ref 26 at $T = 313.15$ K.

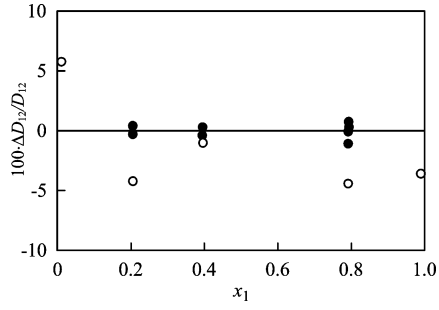

Figure 6. Fractional deviations $\Delta D_{12} = D_{12}(\text{exp}) - D_{12}(\text{corr})$ of the experimental mass diffusion coefficient D_{12}(exp) of acetone + carbon tetrachloride from values D_{12}(corr) obtained with the correlation eq 22 with the coefficients in Table 3. ●, present work at $T = 298.15$ K; ○, ref 27 at $T = 298.15$ K.

Table 3. Concentration Dependence of Mass Diffusion Coefficient D_{12} of Cellulose Acetate Butyrate in Methyl Ethyl Ketone Solutions Determined by the Soret Forced Rayleigh Scattering Method at $T = 298.15$ K

system (1 + 2)	w_1[a]	T/K	$D_{12}/10^{-10}$ m$^2 \cdot$s^{-1}
cellulose acetate butyrate + methyl ethyl ketone	0.050	298.15 ± 0.1	1.49 ± 0.010[b]
	0.100	298.15 ± 0.1	2.04 ± 0.013
	0.200	298.15 ± 0.1	2.70 ± 0.009
	0.300	298.15 ± 0.1	3.16 ± 0.023
	0.400	298.15 ± 0.1	3.31 ± 0.057
	0.500	298.15 ± 0.1	2.85 ± 0.035
	0.600	298.15 ± 0.1	2.09 ± 0.014

[a] Weight fraction of component 1. [b] Standard deviation.

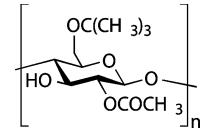

Figure 7. Chemical structure of cellulose acetate butyrate (CAB).

Table 4. Temperature Dependence of Mass Diffusion Coefficient D_{12} of Cellulose Acetate Butyrate in Methyl Ethyl Ketone Solutions Determined by the Soret Forced Rayleigh Scattering

system (1 + 2)	w_1[a]	T/K	$D_{12}/10^{-10}$ m$^2 \cdot$s^{-1}
cellulose acetate butyrate + methyl ethyl ketone	0.100	293.15 ± 0.1	1.90 ± 0.010[b]
		303.15 ± 0.1	2.13 ± 0.015
		312.15 ± 0.1	2.42 ± 0.008
		331.15 ± 0.1	2.73 ± 0.012
	0.200	293.15 ± 0.1	2.56 ± 0.016
		303.15 ± 0.1	2.93 ± 0.019
		313.15 ± 0.1	3.32 ± 0.022
		322.15 ± 0.1	3.75 ± 0.037
	0.300	293.15 ± 0.1	2.95 ± 0.013
		303.15 ± 0.1	3.41 ± 0.026
		312.15 ± 0.1	3.91 ± 0.051
		323.15 ± 0.1	4.30 ± 0.080

[a] Weight fraction of component 1. [b] Standard deviation.

Table 5. Values of Coefficients b_{ij} in Equation 23

j	$i = 0$	$i = 1$	$i = 2$
0	$6.4635 \cdot 10^{-11}$	$7.4648 \cdot 10^{-10}$	$-9.6405 \cdot 10^{-10}$
1	$1.2598 \cdot 10^{-12}$	$1.8454 \cdot 10^{-11}$	$-2.3561 \cdot 10^{-11}$

W. The maximum temperature amplitude $\Delta T(t_h)$ was calculated to be less than 0.01 K; the mean temperature rise $T_m(t_h)$ was less than 0.5 K; and the concentration amplitude $\Delta c(t_h)$ was smaller than 10^{-5}. By taking into account the following source of uncertainty—the determination of decay time constant (0.5 % to 3 % depending on samples), the measurement of fringe spacing (within 0.8 %), the concentration of sample, and the temperature of sample—the expanded ($k = 2$) uncertainty in mass diffusion coefficient is estimated to be ± 1.9 % for (toluene + *n*-hexane), ± 4.6 % for (ethanol + benzene), and ± 2.4 % for (acetone + carbon tetrachloride).

To compare the present experimental results with other experimental data obtained by different methods, we tentatively correlated our raw data together with other experimental data which cover the same temperature and concentration ranges as ours because there is no recommended correlation for liquid mass diffusion coefficient. We fitted the above-mentioned

experimental data for three mixtures to a second-order polynomial in concentration and a first-order polynomial in temperature

$$D_{12}(x_1, T) = \sum_{i=0}^{2}\left(\sum_{j=0}^{1} a_{ij}(T - 273.15)^j\right)x_1^i \qquad (22)$$

where D_{12} is the mass diffusion coefficient in $m^2 \cdot s^{-1}$; T is the temperature in K; and x_1 is the mole fraction of component 1. The optimum values of a_{ij} are given in Table 2. Figure 4 shows the relative deviations of the experimental results of toluene + *n*-hexane from the correlation of eq 22 at $T = 298.15$ K. The data of Ghai et al.[24] using a diaphragm cell, Li et al.[25] using dynamic light scattering, and Zhang et al.[26] using steady-state optical beam deflection mutually agree within 2 %. On the other hand, the present results differ by (8 to 12) % with those previous data with maximum deviations at $x_1 = 0.25$ and 0.75, whereas the equimolar concentration agreement between the four sets of experimental data obtained with completely different methods seems quite reasonable. Figures 5 and 6 compare the present results for (ethanol + benzene) and (acetone + carbon tetrachloride), respectively, with the data of Anderson et al.[27] obtained by a Mach−Zehender-type diffusiometer. In both cases, even though Anderson et al.[27] did not provide any uncertainty assessment, the relative deviations between the present dada and their data[27] are almost within ± 5 % except for the low- and high-concentration regions. Even though we have been unable to identify the source of systematic differences in the case of (toluene + *n*-hexane), by summing up the above-mentioned comparisons of the present S-FRSM data with data measured by different techniques for the mass diffusion coefficient of three organic liquid mixtures, it may be possible to conclude that the Soret forced Rayleigh scattering method is capable of measuring the diffusion coefficients of organic liquid mixtures with an estimated uncertainty of ± 2 % to ± 5 % depending on the sample.

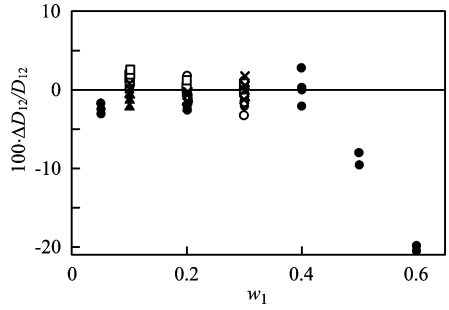

Figure 8. Fractional deviations $\Delta D_{12} = D_{12}(\text{exp}) - D_{12}(\text{corr})$ of the present experimental mass diffusion coefficient $D_{12}(\text{exp})$ of cellulose acetate butyrate (CAB) + methyl ethyl ketone (MEK) from values $D_{12}(\text{corr})$ obtained from the correlation in eq 23 with the coefficients in Table 5. □, $T = 293.15$ K; ●, $T = 298.15$ K; ▲, $T = 303.15$ K; ×, $T = 313.15$ K; ○, $T = 322.15$ K.

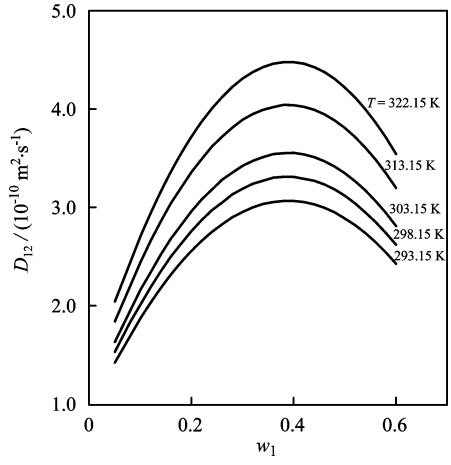

Figure 9. Mass diffusion coefficient of cellulose acetate butyrate (CAB) + methyl ethyl ketone (MEK) solutions calculated by eq 23.

Materials. The methyl ethyl ketone (MEK (desiccated), $CH_3COC_2H_5$) used in the present measurement was supplied by Wako Pure Chemical Industries, Ltd. with a mass fraction purity better than 99 % and cellulose acetate butyrate (CAB, chemical structure is shown in Figure 7) from Eastman Chemical Ltd. ($M_w = 40000$, $M_w/M_n = (2.5$ to $3.0)$, CAB-531). The polydispersity of this commercially available CAB depends on its production lot. Therefore it should be mentioned that the diffusion coefficients of CAB/MEK obtained in the present study are averaged values corresponding to its molecular weight distribution. For the preparation of CAB in MEK solutions (CAB mass fractions of 0.05, 0.10, 0.20, and 0.30) measured in the present work, we simply dissolved CAB in MEK (total sample weight of about 100 g) and stirred well. However, in the case of solutions of higher concentration (CAB mass fractions of 0.40, 0.50, and 0.60) whose viscosity became significantly high, we no longer were able to use the normal mixing recipe. Instead, we employed a recipe to condense a thin solution by evaporating MEK up to the prescribed amount to prepare higher-concentration solutions. During the preparation of these solutions, we continuously rotated and vibrated the sample container to achieve homogeneous mixing without introducing small air bubbles to a maximum extent. All the CAB/MEK solutions were doped with 0.4 $g \cdot L^{-1}$, as in the case of organic solutions.

Results and Discussions

The experimental data for the mass diffusion coefficient of CAB/MEK solutions are listed in Tables 3 (concentration dependence at $T = 298.15$ K) and 4 (temperature dependence for three CAB concentrations). The values listed in the tables are averages of two to five measurements at the same temperature under atmospheric pressure. The fringe spacing selected was (4.18 and 6.99) μm, and the heating pulse duration time of the argon−ion laser was 10 ms with an output power of (1.4 to 2.0) W. The expanded ($k = 2$) uncertainty in the mass diffusion coefficient for CAB/MEK solutions was estimated to be ± 3.6 %.

The present mass diffusion coefficient data for CAB/MEK solutions were correlated by means of the following equation

$$D_{12}(w_1, T) = \sum_{i=0}^{2}\left(\sum_{j=0}^{1} b_{ij}(T - 273.15)^j\right)w_1^i \qquad (23)$$

where D_{12} represents the mass diffusion coefficient, T the temperature, and w_1 the mass fraction of CAB. It may be worth mentioning that we relatively reduced the weighting factor of the data at $w_1 = 0.5$ and 0.6 for the least-squares fitting because at $w_1 = 0.5$ and 0.6 there was the deterioration of uncertainty of mass diffusion coefficient, and also it was difficult to represent the concentration dependence at the high concentration region by the simple practical eq 23 with a second-order polynomial in weight fraction. The coefficients b_{ij} that give the best representation of the present results are shown in Table 5. Since no other experimental data exist for CAB/MEK solutions in the literature, Figure 8 contains the plots of relative deviations of only our raw experimental data from eq 23. Equation 23

reproduces the entire body of experimental results within a standard deviation of ± 1.5 % in the mass fraction range from 0.05 to 0.60 of CAB and in the temperature range from (293.15 to 323.15) K. As can be seen from Figure 8, at the high concentration region, $w_1 = 0.5$ and 0.6, the systematic negative deviations reach −20 %. This is due to the fact that the scattering light from the sample significantly increased in the case of concentrated solutions, which can entrain invisible small air bubbles. Such an increase in scattered light signals deteriorates the decay time constants of the diffracted beam. Consequently, the uncertainty of the mass diffusion coefficient at $w_1 = 0.5$ and 0.6 might be as high as ± 10 % to ± 15 %. Figure 9 shows the behavior of mass diffusion coefficients of CAB/MEK solutions calculated by eq 23 for practical applications at a wide range of temperatures and concentrations.

Acknowledgment

The authors acknowledge Dr. Yasuyuki Yamamoto (Advanced Industrial Science and Technology) for his design and manufacture of the experimental apparatus and Dr. Kazukiro Oki (FUJIFILM Co.) for his supply and preparation of the samples.

Literature Cited

(1) Oki, K.; Nagasaka, Y. Advances in ripplon surface laser-light scattering measurement for highly viscous polymer-solvent system. *Int. J. Thermophys.* **2008**, online No. 38.
(2) Oki, K.; Nagasaka, Y. Dynamic observation of the behavior of the surface of liquid films of polymer-organic solvent system by ripplon surface laser-light scattering method. *Jpn. J. Chem. Eng.* **2008**, *34*, 587–593.
(3) Alsoy, S.; Duda, J. L. Modeling of multicomponent drying of polymer films. *AIChE J.* **1999**, *45*, 896–905.
(4) Pollak, T.; Köhler, W. Critical assessment of diffusion coefficients in semidilute to concentrated solutions of polystyrene in toluene. *J. Chem. Phys.* **2009**, *130*, 124905.
(5) Zielinski, J. M.; Duda, J. L. Predicting polymer/solvent diffusion coefficients using free-volume theory. *AIChE J.* **1992**, *38*, 405–415.
(6) Thyagarajan, K.; Lallemand, P. Determination of the thermal diffusion ratio in a binary mixture by forced Rayleigh scattering. *Opt. Commun.* **1978**, *26*, 54–57.
(7) Pohl, D. W. First stage spinodal decomposition observed by forced Rayleigh scattering. *Phys. Lett.* **1980**, *77A*, 53–54.
(8) Köhler, W. Thermal diffusion in polymer solutions as observed by forced Rayleigh scattering. *J. Chem. Phys.* **1993**, *98*, 660–668.
(9) Köhler, W.; Rossmanith, P. Aspects of thermal diffusion forced Rayleigh scattering: Heterodyne, active phase tracking, and experimental constraints. *J. Phys. Chem.* **1995**, *99*, 5838–5847.
(10) Butenhoff, T. J.; Goemans, G. E.; Buelow, S. J. Mass diffusion coefficients and thermal diffusivity in concentrated hydrothermal $NaNO_3$ solutions. *J. Phys. Chem.* **1996**, *100*, 5982–5992.
(11) Nagasaka, Y.; Hatakeyama, T.; Okuda, M.; Nagashima, A. Measurement of the thermal diffusivity of liquids by the forced Rayleigh scattering method: Theory and experiment. *Rev. Sci. Instrum.* **1988**, *59*, 1156–1168.
(12) Nagasaka, Y.; Nagashima, A. Measurement of the thermal diffusivity of molten KCl up to 1000 °C by the forced Rayleigh scattering method. *Int. J. Thermophys.* **1988**, *9*, 923–931.
(13) Hayashida, K.; Nagasaka, Y. Measurement of mutual diffusion coefficient by the Soret forced Rayleigh scattering method (1st Report, Examination of the method and measurement of polymer solutions). *Trans. Jpn. Soc. Mech. Eng.* **1997**, *B63*, 276–281.
(14) Yamamoto, Y.; Nagasaka, Y. Development of the Soret forced Rayleigh scattering method for measurement of mass diffusion coefficient (1st Report, Development of the measurement system and measurement of the fullerene in solution). *Trans. Jpn. Soc. Mech. Eng.* **2006**, *B72*, 709–714.
(15) Yamamoto, Y.; Nagasaka, Y. Development of the Soret forced Rayleigh scattering method for measurement of mass diffusion coefficient (2nd Report, Theoretical analysis of systematic effect of experimental parameters). *Trans. Jpn. Soc. Mech. Eng.* **2006**, *B72*, 715–722.
(16) *Japanese Patent Laid-open Publication No. 2000−203136*.
(17) *Japanese Patent Publication No. 4004886*.
(18) *Japanese Patent Laid-open Publication No. 2007−241125*.
(19) de Groot, S. R.; Mazur, P. *Non-equilibrium thermodynamics*; Dover: New York, 1983; Chapter *11*, p 276.
(20) Koyama, J.; Nishihara, H. *Optical wave electronics*; Corona: Tokyo, 1978; Chapter *4*, p 122.
(21) Johnston, T. F., Jr.; Fleischer, J. M. Calibration standard for laser beam profilers: method for absolute accuracy measurement with a Fresnel diffraction test pattern. *Appl. Opt.* **1996**, *35*, 1719–1734.
(22) Yamamoto, Y.; Niwa, M.; Nagasaka, Y. Measurement of concentration dependence of mutual diffusion coefficient in polymer solution using the Soret forced Rayleigh scattering method. *Proc. 16th Symposium on Thermophysical Properties*, 2006, CD-ROM.
(23) Wakeham, W. A.; Nagashima, A.; Sengers, J. V. Reference Data. In *Experimental Thermodynamics III, Measurement of the Transport Properties of Fluids*; Wakeham, W. A., Nagashima, A., Sengers, J. V., Eds.; Blackwell Scientific, 1991; Chapter *13*, pp 439−451.
(24) Ghai, R. K.; Dullien, F. A. L. Diffusivities and viscosities of some binary liquid nonelectrolytes at 25°. *J. Phys. Chem.* **1974**, *78*, 2283–2291.
(25) Li, W. B.; Sengers, J. V.; Gammon, R. W.; Segre, P. N. Measurement of transport properties of liquids with equilibrium and nonequilibrium Rayleigh scattering. *Int. J. Thermophys.* **1995**, *16*, 23–31.
(26) Zhang, K. J.; Briggs, M. E.; Gammon, R. W.; Sengers, J. V. Optical measurement of the Soret coefficient and the diffusion coefficient of liquid mixtures. *J. Chem. Phys.* **1996**, *104*, 6881–6892.
(27) Anderson, D. K.; Hall, J. R.; Babb, A. L. Mutual diffusion in nonideal binary liquid mixtures. *J. Phys. Chem.* **1958**, *62*, 404–408.

Received for review March 6, 2009. Accepted May 11, 2009. The work described in this article has been supported in part by a Grant-in-Aid for Scientific Research (S) (No. 19106004) from the Ministry of Education, Culture, Sports, and Technology of Japan.

JE900242E